ELSEVIER

Chemical Engineering Journal 140 (2008) 509–520

Chemical Engineering Journal

www.elsevier.com/locate/cej

Phase stability analysis using the PC-SAFT equation of state and the tunneling global optimization method

Dan Vladimir Nichita [a,*], Fernando García-Sánchez [b], Susana Gómez [c]

[a] *UMR 5150 CNRS, Laboratoire des Fluides Complexes, Université de Pau et des Pays de l'Adour, B.P. 1155, 64013 Pau Cedex, France*

[b] *Laboratorio de Termodinámica, Programa de Ingeniería Molecular, Instituto Mexicano del Petróleo. Eje Central Lázaro Cárdenas 152, 07730 México, D.F., Mexico*

[c] *Instituto de Investigación en Matemática Aplicada y Sistemas, Universidad Nacional Autónoma de México, Apdo. Postal 20-726, 01000 México, D.F., Mexico*

Received 25 July 2007; received in revised form 20 November 2007; accepted 27 November 2007

Abstract

Phase stability calculation is a very important topic in phase equilibrium modeling. Usually the phase stability problem is solved by minimization of the tangent plane distance (TPD) function, the sign of the objective function at its global minimum indicating the state of the mixture at given conditions. The TPD function is non-convex and may be highly non-linear, many phase stability problems being really challenging. The tunneling global optimization method had been successfully used for solving a variety of phase equilibrium problems, including stability, with cubic equations of state (EoS). In this work, we test the ability of the tunneling method to solve the phase stability problem for more complex EoS like PC-SAFT. Calculations are performed for several benchmark problems, for mixtures of non-associating molecules, from binaries to multicomponent. In one example, the mixture contains hydrogen sulphide, for which the three parameters required by the PC-SAFT EoS were unavailable in the literature. These parameters, as well as the binary interaction parameter (BIP) between hydrogen sulphide and methane, were calculated based on experimental data.

Keywords: Phase stability; Tangent plane distance; Global optimization; Tunneling; PC-SAFT equation of state

1. Introduction

Phase stability analysis calculations represent an important subproblem of phase equilibrium calculations. It is intensively used in research and industrial applications for chemical process simulation, design and optimization, hydrocarbon reservoir engineering, etc. Phase stability analysis can asses the state of a mixture at given conditions; it is very useful for initialization of phase split calculations, as well as for their validation.

The criteria for thermodynamic stability were first set by Gibbs [1]; Baker et al. [2] provided a comprehensive analysis of these criteria, while Michelsen [3] proposed the implementation of the TPD function, which is currently the most widely used.

The dimensionless TPD function, Michelsen [3], has the form

$$\bar{D}(\boldsymbol{x}) = \frac{D(\boldsymbol{x})}{RT} = \sum_{i=1}^{\mathrm{nc}} x_i(\ln\ f_i(\boldsymbol{x}) - \ln\ f_i(\boldsymbol{z})) \tag{1}$$

where f_i is the fugacity of component i, $\boldsymbol{z} = (z_1,\ldots,z_{\mathrm{nc}})^{\mathrm{T}}$ is the composition of the feed whose stability is assessed.

The vector of primary variables is $\boldsymbol{x} = (x_1,\ldots,x_{\mathrm{nc}-1})^{\mathrm{T}}$ containing the mole fractions in the trial phase; here we have considered the mole fraction of component "nc" as dependent variable

$$x_{\mathrm{nc}} = 1 - \sum_{i=1}^{\mathrm{nc}-1} x_i \tag{2}$$

The problem can be formulated as an optimization problem or as the resolution of non-linear system of equations. The minimization problem to be solved is:

* Corresponding author. Tel.: +33 5 5940 7685; fax: +33 5 5940 7725.
E-mail address: dnichita@univ-pau.fr (D.V. Nichita).

1385-8947/$ – see front matter © 2007 Elsevier B.V. All rights reserved.
doi:10.1016/j.cej.2007.11.036

Nomenclature

a	reduced Helmholtz free energy
A	Helmholtz free energy (J)
d	temperature-dependent segment diameter (Å)
D	tangent plane distance function
$\bar{D}$	dimensionless tangent plane distance function
f_i	fugacity of component i
F	objective function for the tunneling method
g^{hc}	average radial distribution function of hard-chain fluid
$g^{\mathrm{hc}}_{\alpha\beta}$	site–site radial distribution function of hard-chain fluid
I_1, I_2	integral functions; defined by Eq. (15) and (16)
k	Boltzmann constant (J/K)
k_{ij}	binary interaction parameter between components i and j
m	number of segments per chain
$\bar{m}$	mean segment number in the system
n	umber of independent variables
nc	number of components
p	pressure (bar)
R	universal gas constant
S_{BP}	objective function (BP pressure method)
S_{Flash}	objective function (Flash method)
T	temperature (K)
T	tunneling function
$T_{\mathrm{c}}(x)$	classical tunneling function
$T_{\mathrm{e}}(x)$	exponential tunneling function
x	independent variable (Section 3)
x_i	mole fraction of component i in the trial phase
x_i	liquid mole fraction of component i, Eq. (40) and (41)
x_{m}	stationary points
x_{tu}	feasible point in another valley of the objective function
y_i	mole fraction of component i in the trial phase
z_{i}	feed composition, component i
Z	compressibility factor

Greek letters

ζ_n	defined by Eq. (7), $n = 0, 1, 2, 3$ (Å^{n-3})
η	packing fraction; $\eta = \zeta_3$
λ_{m}	strength of the pole at the point x_{m}
ρ	total number density of molecules (1/Å^3)
σ	segment diameter (Å)
σ_P	standard percent relative deviation in pressure
σ_x	standard percent deviation in liquid mole fraction
σ_y	standard percent deviation in vapor mole fraction
φ_i	fugacity coefficient of component i

Superscripts

calc	calculated property
disp	contribution due to dispersive attraction
hc	residual contribution of hard-chain system
hs	residual contribution of hard-sphere system
res	residual property
T	transposed
*	at stationary points
ν	iteration level

Subscripts

G	at the global minimum
i, j, k	component index

Find

$$\min \ \bar{D}(\boldsymbol{x})$$

s.t.

$$0 \le x_i \le 1; \quad i = 1, \ \mathrm{nc} - 1$$

A phase is stable if all stationary points of D are non-negative, that is, the value of the TPD function at the global minimum is zero (the trivial solution $\boldsymbol{x} \equiv \boldsymbol{z}$ is always a stationary point of D); a negative value of D at a stationary point indicates that the mixture is unstable and will split into two or more phases at given conditions.

The TPD surface is non-convex and may be highly non-linear; it has many stationary points (including trivial solutions and non-physical solutions) which can be local minima or saddle points. Even though they may be very fast, local solution methods are initialization dependent, and may converge to undesired stationary points different from the putative global minimum. Local methods are finding a single stationary point for a given initial guess; in a multiphase context, starting from many different initial guesses still does not offer the guarantee that the global minimum was found [3].

The TPD analysis requires the component fugacity (or chemical potential) at given pressure, temperature and feed composition. As mentioned, minimization of the TPD function is a difficult problem itself; additional complexity may be added by the thermodynamic model.

Mainly in the last decade, a variety of global optimization methods have been used to solve the global stability problem: homotopy continuation [4], branch and bound [5–8], Newton-interval [9–12], simulated annealing [13], space search [14], tunneling [15–19]. Some of these methods are designed to find all the stationary points, while others are computing only the global minimum. They were applied to different thermodynamic models, from relatively simple (such as cubic EoS) to very complex ones.

In our previous work on phase stability analysis we have used the gradient-based tunneling global optimization method together with a general form of cubic EoS. Different formulations of the TPD criterion have been used, including those based on reduced variables [16], component molar densities as primary variables [18], or using a modified objective function [19].

The aim of this work is to study the ability of the tunneling method when complex thermodynamic models are used.

Starting from the original statistical association fluid theory (SAFT) EoS proposed by Chapmann et al. [20], a variety of equations of state were proposed; see for instance the comprehensive review by Müller and Gubbins [21]. In this work we use the perturbed-chain SAFT (PC-SAFT) EoS, as introduced by Gross and Sadowski [22].

In this work, we are focusing on mixtures containing hydrocarbon components and hydrogen sulphide, carbon dioxide and nitrogen, such as naturally occurring reservoir fluids. The PC-SAFT EoS proved to give good results for synthetic hydrocarbon mixtures [23].

Petroleum reservoir mixtures (hydrocarbons + classical contaminants, except water) can be treated without association, considering only the dispersive term in the PC-SAFT EoS.

The paper is structured as follows: we first briefly present the PC-SAFT EoS, then we describe an up-to-date version of the tunneling global optimization method as implemented in this work (we stress on handling tolerances for generating the initial points in the tunneling phase, which are crucial for the robustness of the method); finally, the reliability and efficiency of the tunneling method are tested on several difficult numerical examples. The component parameters and the BIP between methane and hydrogen sulphide required by one example are calculated by matching experimental data available in the literature.

2. The PC-SAFT equation of state

In the PC-SAFT equation of state [22], the molecules are conceived to be chains composed of spherical segments, in which the pair potential for the segment of a chain is given by a square-well potential suggested by Chen and Kreglewski [24]. Non-associating molecules are characterized by three pure component parameters: the number of segments per chain m, the depth of the potential ε, and the temperature independent segment diameter σ. In this section, we will only summarize the main expressions of the PC-SAFT equation of state; full details can be found in the original paper by Gross and Sadowski [22].

The PC-SAFT equation of state is written in terms of the Helmholtz free energy A that, for a multicomponent mixture of non-associating chains, consists of a hard-chain reference contribution and a perturbation contribution to account for the attractive interactions. In terms of reduced quantities, this equation can be expressed as

$$\tilde{a}^{\mathrm{res}} = \tilde{a}^{\mathrm{hc}} + \tilde{a}^{\mathrm{disp}} \tag{3}$$

where $a = A/nkT$.

It should be noted that the contribution due to association is not included in this work since we are dealing with non-associating systems. Therefore, only dispersive attractions are considered.

The hard-chain reference contribution is given by

$$\tilde{a}^{\mathrm{hc}} = \bar{m}\,\tilde{a}^{\mathrm{hs}} - \sum_{i=1}^{\mathrm{nc}} x_i (m_i - 1) \ln\, g_{ii}^{\mathrm{hs}}(\sigma_{ii}) \tag{4}$$

where $\bar{m}$ is the mean segment number in the mixture

$$\bar{m} = \sum_{i=1}^{\mathrm{nc}} x_i m_i \tag{5}$$

The Helmholtz free energy of the hard-sphere fluid is given on a per-segment basis

$$\tilde{a}^{\mathrm{hs}} = \frac{1}{\zeta_0}\left[\frac{3\zeta_1\zeta_2}{1-\zeta_3} + \frac{\zeta_2^3}{\zeta_3(1-\zeta_3)^2} + \left(\frac{\zeta_2^3}{\zeta_3^2} - \zeta_0\right)\ln(1-\zeta_3)\right] \tag{6}$$

with ζ_n defined as

$$\zeta_n = \frac{\pi}{6}\rho \sum_{i=1}^{\mathrm{nc}} x_i m_i d_i^n; \quad n = 0, 1, 2, 3 \tag{7}$$

and the radial distribution function of the hard-sphere fluid given by

$$g_{ij}^{\mathrm{hs}} = \frac{1}{1-\zeta_3} + \left(\frac{d_i d_j}{d_i + d_j}\right)\frac{3\zeta_2}{(1-\zeta_3)^2} + \left(\frac{d_i d_j}{d_i + d_j}\right)^2 \frac{2\zeta_2^2}{(1-\zeta_3)^3}; \quad i,\ j = 1,\ \mathrm{nc} \tag{8}$$

The temperature-dependent segment diameter d_i of component i is given by

$$d_i = \sigma_i\left[1 - 0.12\,\exp\left(-3\frac{\varepsilon_i}{kT}\right)\right] \tag{9}$$

where k is the Boltzmann constant and T is the absolute temperature.

The dispersion contribution to the Helmholtz free energy is given by

$$\tilde{a}^{\mathrm{disp}} = -2\pi\rho\, I_1(\eta, \bar{m})\,\overline{m^2\varepsilon\sigma^3} - \pi\rho\,\bar{m}\left(1 + Z^{\mathrm{hc}} + \rho\frac{\partial Z^{\mathrm{hc}}}{\partial\rho}\right)^{-1} I_2(\eta, \bar{m})\,\overline{m^2\varepsilon^2\sigma^3} \tag{10}$$

where Z^{hc} is the compressibility factor of the hard-chain reference contribution, and

$$\overline{m^2\varepsilon\sigma^3} = \sum_{i=1}^{\mathrm{nc}}\sum_{j=1}^{\mathrm{nc}} x_i x_j m_i m_j \left(\frac{\varepsilon_{ij}}{kT}\right)\sigma_{ij}^3 \tag{11}$$

$$\overline{m^2\varepsilon^2\sigma^3} = \sum_{i=1}^{\mathrm{nc}}\sum_{j=1}^{\mathrm{nc}} x_i x_j m_i m_j \left(\frac{\varepsilon_{ij}}{kT}\right)^2\sigma_{ij}^3 \tag{12}$$

The parameters for a pair of unlike segments are obtained by using conventional Lorentz–Berthelot combining rules

$$\varepsilon_{ij} = \sqrt{\varepsilon_i\varepsilon_j}(1 - k_{ij}) \tag{13}$$

$$\sigma_{ij} = \frac{1}{2}(\sigma_i + \sigma_j) \tag{14}$$

where k_{ij} is a binary interaction parameter between components i and j which is introduced to correct the segment–segment interactions of unlike chains.

The terms $I_1(\eta, \bar{m})$ and $I_2(\eta, \bar{m})$in Eq. (10) are substituted by simple power series in density

$$I_1(\eta, \bar{m}) = \sum_{i=0}^{6} a_i(\bar{m})\eta^i \tag{15}$$

$$I_2(\eta, \bar{m}) = \sum_{i=0}^{6} b_i(\bar{m})\eta^i \tag{16}$$

where the coefficients a_i and b_i depend on the chain length as given in Gross and Sadowski [22].

The density to a given system pressure p^{sys} is determined iteratively with the Newton–Raphson method by adjusting the reduced density η until $p^{\text{calc}} = p^{\text{sys}}$. For a converged value of η, the number density of molecules ρ (given in Å^{-3}) is calculated from

$$\rho = \frac{6}{\pi}\eta\left(\sum_{i=1}^{\text{nc}} x_i m_i d_i^3\right)^{-1} \tag{17}$$

The molar density ρ can be expressed in different units such as kmol m^{-3} by using Avogadro's number and appropriate conversion factors.

The compressibility factor Z is calculated from the relation

$$Z = 1 + \eta\left(\frac{\partial \tilde{a}^{\text{res}}}{\partial \eta}\right)_{T,x_i} = 1 + Z^{\text{hc}} + Z^{\text{disp}} \tag{18}$$

The pressure can be calculated in SI units of $\text{Pa} = \text{N/m}^2$ by applying the relation

$$p = Z\,kT\rho\left(10^{10}\frac{\text{Å}}{\text{m}}\right)^3 \tag{19}$$

The fugacity coefficient $\varphi_i(T,p)$; $i, j = 1$, nc is related to the residual chemical potential according to

$$\ln\,\varphi_i = \frac{\mu_i^{\text{res}}(T, v)}{NkT} - \ln\,Z \tag{20}$$

where $\mu_i^{\text{res}}$is obtained from

$$\frac{\mu_i^{\text{res}}(T, v)}{NkT} = \tilde{a}^{\text{res}} + (Z-1) + \left(\frac{\partial\,\tilde{a}^{\text{res}}}{\partial x_i}\right)_{T,v,x_{j\neq i}} - \sum_{k=1}^{\text{nc}}\left[x_k\left(\frac{\partial \tilde{a}^{\text{res}}}{\partial x_k}\right)_{T,v,x_{j\neq k}}\right] \tag{21}$$

In Eq. (19), partial derivatives with respect to mole fractions are calculated regardless of the summation relation $\sum_{i=1}^{\text{nc}} x_i = 1$.

3. The tunneling global optimization method

3.1. The tunneling method

The code used in this work is based on the classical Levy and Montalvo [25] and exponential Barrón–Gómez [26] tunneling methods, modified to deal with bounded problems to find global optima of non-linear smooth functions, subject to bounds on the variables, that is

$$\begin{aligned} &F_{\text{G}}^* \equiv \inf\{F(x)\} \\ &\text{subject to } x \in B \end{aligned} \tag{22}$$

where $B = \{x \in R^n:\ l \le x \le u;\ l,\ u \in R^n;\ i = 1,n\}$ is the feasible region and $F: B \to R: F \in C^2$.

The basic idea of these methods is to *tunnel* from one valley of the objective function to another, to find a sequence of local minima with decreasing function values, $F(x_1^*) \ge F(x_2^*) \ge \cdots \ge F(x_{\text{G}}^*)$, where x_{G}^* is the global minimum of $F(x)$ and $x_i \neq x_j$ for $i \neq j$, ignoring the local minima with larger objective function values than the ones already found (up to a tolerance given by the user). This characteristic of "ignoring" minima makes the algorithm more efficient and faster than other general purpose methods like simulated annealing, random search, clustering and genetic algorithms (see Gómez et al. [27]).

The tunneling method has two phases. In phase 1, the minimization phase, starting from an initial point x_0, finds a local minimum x^* with $F^* = F(x^*)$, using any local bound constrain optimization method. In phase 2, the tunneling phase, a feasible point x_{tu}^* is obtained in another valley with $F(x_{\text{tu}}^*) \le F^*$, which will be taken as the initial point for the subsequent phase 1 (see Fig. 1).

3.2. Minimization phase

Any algorithm designed to solve local optimization problems with bounds on the variables can be used in this phase. We use here a limited-memory quasi-Newton BFGS method [28,29]. The implementation is designed to solve large size problems, but when the problem is of small size (that is, problem dimensionality is from $n = 3$ to $n = 40$) as it is in our case, the method can behave similarly to a normal quasi-Newton, if the number of gradient and step vectors used to update the approximation of the Hessian is taken equal to n (see [30]). In this code the criteria to consider a successful local optimization is given by:

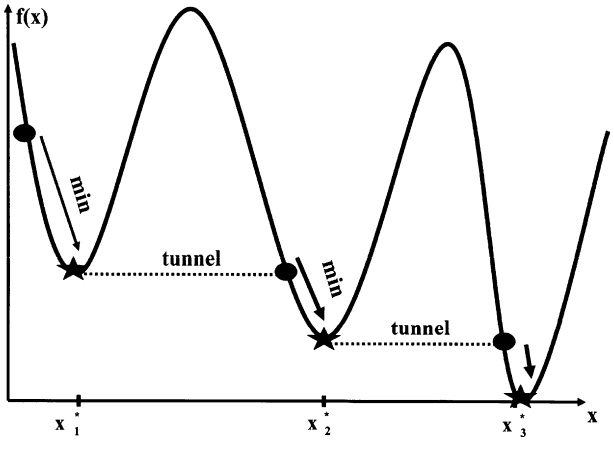

Fig. 1. The basic idea of the tunneling method.

(a) The infinity norm of the projected gradient at the current iteration is sufficiently small:

$$||\text{proj}\, g(x^{\nu+1})||_\infty \leq \text{PGTOL} \tag{23}$$

with PGTOL being a positive small tolerance (less than one) given by the user.

(b) No further improvement in the successive values of the objective function is possible

$$|F^{\nu+1} - F^{\nu}| \leq \text{TOLF}(1 + |F^{\nu+1}|) \tag{24}$$

with $F^{\nu+1} = F(x^{\nu+1})$ and $F^{\nu} = F(x^{\nu})$

In some local optimization codes, TOLF is given by the user. In the case of the code L-BFGS-B used here

$$\text{TOLF} = \text{FACTR} \cdot \text{epsmch} \tag{25}$$

with epsmch being the machine precision which is automatically generated by the code and the user supplies a value FACTR $\in [10^0, 10^{15}]$. Typical values for FACTR on a computer with 15 digits of accuracy in double precision are: FACTR = 1.d + 12 for low accuracy; FACTR = 1.d + 7 for moderate accuracy; FACTR = 1.d + 1 for extremely high accuracy. If the user sets FACTR = 0, the test will stop the algorithm only if the objective function remains unchanged after one iteration.

3.3. Tunneling phase

3.3.1. Tunneling functions

Once a local minimum x^* has been found, we have to solve an inequality problem:

Find the x^*_{tu} such that

$$T(x^*_{\text{tu}}) = F(x^*_{\text{tu}}) - F(x^*) \leq 0, \quad x^*_{\text{tu}} \neq x^* \tag{26}$$

If an x^*_{tu} is found, it would be in another valley.

To solve the inequality problem (26) using gradient type methods, we place a pole at x^* to destroy the minimum, and create a transformed problem using one of the following functions (where $||\cdot||$ is the squared Euclidean norm) (see Fig. 2):

Tunneling function [25]

$$T_{\text{c}}(x) = \frac{F(x) - F(x^*)}{||x - x^*||^{\lambda *}} \tag{27a}$$

Exponential tunneling function [26]

$$T_{\text{e}}(x) = (F(x) - F(x^*))\text{e}^{(\lambda */||x - x^*||)} \tag{27b}$$

The exponential function is generally faster.When $||x - x^*|| > 1$ functions T_{c} and T_{e} become flat slowing the convergence to x^*_{tu}, and thus we need to modify them as follows:

$$T_{\text{e}}(x) = \begin{cases} (F(x) - F(x^*))\text{e}^{(\lambda */||x - x^*||)} & \text{if } ||x - x^*|| < 1 \\ F(x) - F(x^*) & \text{if } ||x - x^*|| \geq 1 \end{cases} \tag{28}$$

The same applies for the classical tunneling function. For both functions, λ^* is the *strength of the pole* and to guarantee

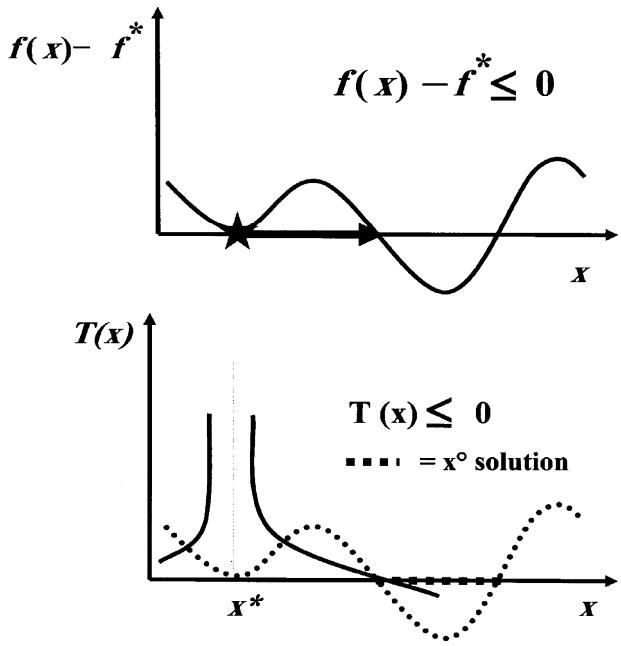

Fig. 2. Generating a new feasible initial estimate by placing a pole and destroying the minimum already found.

continuity and differentiability at points with $||x - x^*|| = 1$, we use the ramp function introduced in Levy and Montalvo [25].

Solving problem (26) now consists in finding x^*_{tu} such that

$$T_{\text{c}}(x^*_{\text{tu}}) \leq 0 \;\text{ or }\; T_{\text{e}}(x^*_{\text{tu}}) \leq 0 \tag{29}$$

We can take Newton type descent directions to solve this inequality problem since $T(x)$ is smooth for $x \neq x^*$ and thus it is possible to use the same algorithm used in the minimization phase that produce descent directions, with appropriate stopping conditions to solve the inequality problem (29).

As the original objective function is a general non-linear function only assumed to belong to C^2 for $x \in B$, it could have many local and global minima and convergence to other minima with the same (and so far the best) value F^* of the objective function (at the same level) is possible, that is, with $F(x^*_i) = F(x^*_{i-1}) = F^*$. Those would be acceptable solutions for problem (26) satisfied at the equality. Then, in order to avoid going back to those minima at the same level already found, during the tunneling phase the poles set at each minimum are preserved until a better lower value of the objective function is found. When this happens, the poles are no longer needed as the algorithm will never accept a point with $F(x) > F(x^*)$. The tunneling functions (27a) and (27b) take the form:

$$T_{\text{c}}(x) = \frac{F(x) - F(x^*)}{\prod_{i=1}^{t} ||x - x^*_i||^{\lambda^*_i}} \tag{30a}$$

and

$$T_{\text{e}}(x) = (F(x) - F(x^*)) \prod_{i=1}^{t} \text{e}^{(\lambda */||x - x^*||)} \tag{30b}$$

making $t = 1$ as soon as a new minimum is found with a smaller function value than $F(x^*)$.

The specific algorithm is as follows:
Given an initial guess x_0 until convergence do

Phase 1—local minimization
From an initial point x^0
Find $arg \min_{x \in B} F(x) = x^*$
Phase 2—tunnelization
From an initial point x^0_{tu} in a neighborhood of x^*
Find x^*_{tu} such that $T(x^*_{tu}) \leq 0$ and $x^*_{tu} \in B$ using the local optimization routine used in phase 1 to generate descent directions and acceptable step lengths for $T(x)$.
Set $x^*_{tu} \rightarrow x^0$, and go to phase 1.

3.3.2. Initial point for the tunneling phase

Once a local minimum x^* has been found, we need to generate an initial point x^0_{tu} to start the tunneling phase. This point is generated along a random direction in a neighborhood of x^*, to preserve local information, as follows:

$$x^0_{tu} = x^* + \varepsilon_1 \frac{r}{||r||} \tag{31}$$

where $r^T = (r_1, \ldots, r_n)$ with $r_i \in (-1, 1)$ for $i = 1, n$, random with normal distribution.

Parameter ε_1 is the minimum distance from x^* to x^0_{tu} and must be selected in such a way, that the new initial point x^0_{tu} is in a neighbourhood of x^* and is related to the desired precision in x^*. It has to be carefully selected to avoid a conflict with other tolerances of the method (as the one that decides that another point is a minimum at the same level). This can be clearer with the following analysis:

It is known (see Gill et al. [31]) that for a well-conditioned problem, satisfaction of Eq. (24) implies that

$$||x^{\nu+1} - x^{\nu}|| \leq \sqrt{\text{TOLF}} \left(1 + ||x^{\nu+1}||\right) \tag{32}$$

If x^*_e represents the exact minimum and $x^* = x^{\nu+1}$ is an approximated, then the right-hand-side of (13) is also an upper bound for the distance from x^*_e to x^*, *i.e.*:

$$||x^*_e - x^{\nu}|| \leq \sqrt{\text{TOLF}} \left(1 + ||x^*||\right) \tag{33}$$

under the assumption stated. In order not to take any other possible minimum within the neighborhood of x^*_e of radius $\sqrt{\text{TOLF}} * (1 + ||x^*||)$, the initial point for the tunneling phase should satisfy.

$$\sqrt{\text{TOLF}} \left(1 + ||x^*||\right) \leq ||x^*_e - x^0_{tu}|| \tag{34}$$

As we only have the approximated minimum and not the exact one, then the distance from x^* to x^0_{tu} should be at least

$$2\sqrt{\text{TOLF}}(1 + ||x^*||) \tag{35}$$

As the condition of a well-conditioned problem that we assume for this derivation is not always satisfied in practice, we relax the bound as

$$\varepsilon_1 = 2(\text{TOLF})^c (1 + ||x^*||) \tag{36}$$

with $c = 1/5$.

This choice for the initial point of the tunneling phase differs from the ones presented in Levy and Montalvo [25] and Barrón and Gómez [26] and is adaptive in the sense that the minimum distance ε_1 depends on the current local minimum to be destroyed.

Tunneling would not be successful (condition (29) has not been satisfied yet) due to any of the following reasons:

(i) A corner of the admissible set has been reached.
(ii) The strength of the pole is greater than a preset maximum value without having obtained a descent direction.
(iii) The maximum number of function evaluations allowed for this phase has been reached.

In any of these cases it is necessary to restart tunneling from another initial point, x^0_{tu}. In our implementation the number of initial points generated in a neighborhood of x^* using Eq. (31) is $2n$, where n is the problem dimension. In order to explore further, we then take initial points generated at random in the whole feasible region until the amount of computing time given by the user is reached. The default value is max(100,5n). If no solution to problem (26) is found for this number of initial points, the algorithm will stop (see Section 3.4).

3.3.3. Mobile poles

As $T(x)$ inherits the multimodality of $F(x)$, the local method used in the tunneling phase could have problems at critical points of $T(x)$. Also, it can find points where the tunneling function values or the iterands cannot be improved (through conditions (23) or (24) on $T(x)$). Here again, to be able to move from this point we place a pole x_m, called *mobile pole*. The tunneling functions (30a) and (30b) are now modified again to finally get

$$T_c(x) = \frac{F(x) - F(x^*)}{\prod_{i=1}^{t} ||x - x^*_i||^{\lambda^*_i}} \frac{1}{||x - x_m||^{\lambda_m}} \tag{37a}$$

and

$$T_e(x) = (F(x) - F(x^*)) \prod_{i=1}^{t} e^{(\lambda * / ||x - x^*_i||)} e^{(\lambda_m / ||x - x_m||)} \tag{37b}$$

where x_m is the position of the mobile pole and λ_m its strength. It is necessary here again to use the ramp function given in Levy and Montalvo [25].

Each time a mobile pole is placed the tunneling function is modified and a descent direction is computed for this new function. Also an initial point in a neighborhood of x_m has to be created to continue the process. This is done as in Section 3.2 and also differs from the original implementation given in Levy and Montalvo [25] and Barrón and Gómez [26].

When the strength of a pole either λ^* or λ_m is increased, it is not necessary to re-evaluate neither the objective function nor its gradient. The same is true if the position of the mobile pole is changed or the mobile pole is turned off, when it is no longer needed.

Table 1
Pure-component parameters of the PC-SAFT equation of state used in this work[a]

Component	M (g/mol)	m	σ (Å)	ε/k (K)
Nitrogen	28.010	1.2053	3.3130	90.96
Carbon dioxide	44.010	2.0729	2.7852	169.21
Methane	16.043	1.0000	3.7039	150.03
Hydrogen sulphide	34.080	1.7563	3.0019	222.12
Ethane	30.070	1.6069	3.5206	191.42
Propane	44.096	2.0020	3.6184	208.11
nC$_5$	72.146	2.6896	3.7729	231.20
nC$_7$	100.203	3.4831	3.8049	238.40
nC$_{10}$	142.285	4.6627	3.8384	243.87

[a] From Gross and Sadowski [22], except parameters for H_2S.

3.3.4. Precision details

The stopping condition for a successful tunneling, that is $T(x_{\text{tu}}^k) \leq 0$, is implemented as follows:

$$F(x_{\text{tu}}^k) - F(x^*) \leq \text{TOLT}(1 + |F(x^*)|) \tag{38}$$

and precision TOLT is to be selected by the user. This parameter is closely related to the tolerance TOLEV for considering minima to be at the same level of the objective function value (for details on these tolerances see Nichita and Gómez [19]).

3.4. General stopping conditions

The algorithm stops when any of the following global criteria is satisfied:

(i) The tunneling phase is unsuccessful: the algorithm was not able to find a point in another valley, starting the search from the number of initial points allowed. The last minimum found is the putative global minimum.
(ii) The given maximum number of function evaluations has been reached.
(iii) If the user has given a lower bound of the objective function and the method has reached that value. The last minimum found is the putative global minimum.
(iv) If the user has given a lower bound of the objective function and all the global minima at that level, required by the user, have been found.

4. Results

Problems 1–5 in this section are benchmark problems for phase stability testing (involving binary and ternary mixtures), taken from Hua et al. [10], and have been also addressed previously with the tunneling method using cubic EoS [15,16,18]. Problem 6 is for a synthetic hydrocarbon mixture of Yarborough [32]. Most of the (T,p,$\mathbf{z}$) points in the numerical experiments are chosen near phase boundaries or critical points, giving difficult problems.

The pure component parameters (m, ε, and σ) used in this work are listed in Table 1. The BIPs of short chain length alkanes (methane and ethane) with heavier hydrocarbon components, and CO_2 BIPs with normal-alkanes were previously obtained [33] by minimizing the sum of squared relative deviations of bubble/dew point pressure and equilibrium data (when available) of binary mixtures. The BIPs between nitrogen and hydrocarbon components are taken from García-Sánchez et al. [34].

We use in all examples very strict tolerances. We consider FACTR = $1.d+2$ corresponding to a high accuracy, and the tolerance associated with the projected norm of the gradient vector PGTOL is set at $1.d-8$. The tunneling method would eventually converge to the global minimum for any initial guess in the feasible region. Here we report results using the two-sided initialization of Michelsen [3], as implemented in [15]. The two initialization types are denoted here as L (for $x_i^{(0)} = z_i K_i$) and V (for $x_i^{(0)} = z_i/K_i$). The equilibrium constants are estimated using Wilson's [35] relation, with pure component critical parameters and acentric factors taken from Reid et al. [36].

4.1. Problem 1: methane–hydrogen sulphide binary mixture

The first problem (first addressed by Michelsen [3] who discussed its difficulty) is for a methane and hydrogen sulphide binary mixture at $p = 40.53$ bar and $T = 190$ K.

The pure component parameters (m, ε, and σ) for H_2S and the BIP between methane and H_2S are not available in the literature. We assume that H_2S behavior can be modeled without taking association into account; H_2S has an intermediate bond energy (Müller and Gubbins [21], see Fig. 1).

We calculate pure component parameters by matching available experimental data (vapor pressure and saturated liquid density) from the triple point to the critical point. The objective function

$$S_{\text{PAR}}(m,\varepsilon,\sigma) = \sum_i^{\text{np}} \left[\left(\frac{P_{\text{V}i}^{\text{exp}} - P_{\text{V}i}^{\text{calc}}(m,\varepsilon,\sigma)}{P_{\text{V}i}^{\text{exp}}} \right)^2 + \left(\rho_{\text{L}i}^{\text{exp}} - \rho_{\text{L}i}^{\text{calc}}(m,\varepsilon,\sigma)\right)^2 \right] \tag{39}$$

where np is the number of experimental points, is minimized using the simplex optimization procedure of Nelder and Mead [37] with convergence accelerated by the Wegstein algorithm [38].

Experimental data (P_{V} and ρ_{L}) are from Kay and Rambosek [39] (20 experimental points in the temperature range from 272.04 K to 373.09 K), and Bierlien and Kay [40] (15 experimental points in the temperature range from 286.43 K to 370.4 K). For lower pressures, we have found only vapor pressure data in Gómez-Nieto and Papadopoulos [41] (15 experimental points in the temperature range from 164.95 K to 213.22 K). For these 15 temperatures, saturated liquid densities from Daubert and Danner [42] were added to the data set; finally, np = 50. The optimum values we have obtained are $m = 1.7563$, $\varepsilon = 3.0019$ Å, $\sigma = 222.12$ K, with standard relative deviations of 2.54% in pressure and 2.85% in density.

The BIP between methane and H_2S is calculated by matching experimental data (bubble points and equilibrium data) from Reamer et al. [43] and Kohn and Kurata [44]

Table 2
Adjustment of the BIP between C_1 and H_2S

Source (method)	np	Temperature range (K)	Pressure range (MPa)	σ_P (%)	σ_y (%)	σ_x (%)	k_{12}
Ref. [43] (BP)	56	277.59–344.26	1.38–13.10	4.7	1.8	–	0.0516
Ref. [43] (Flash)	56	277.59–344.26	1.38–13.10	–	1.5	1.3	0.0429
Ref. [44] (BP)	49	188.70–366.48	1.38–11.03	9.0	2.6	–	0.0648
Ref. [44] (Flash)	49	188.70–366.48	1.38–11.03	–	1.5	0.5	0.0614
Refs. [43,44] (BP)	105	188.70–366.48	1.38–13.10	8.1	2.4	–	0.0600
Refs. [43, 44] (Flash)	105	188.70–366.48	1.38–13.10	–	1.7	1.4	0.0475

The minimum of the following objective functions:

$$S_{\mathrm{BP}} = \sum_{i}^{\mathrm{np}} \left[\left(\frac{P_i^{\mathrm{exp}} - P_i^{\mathrm{calc}}}{P_i^{\mathrm{exp}}} \right)^2 + (y_i^{\mathrm{exp}} - y_i^{\mathrm{calc}})^2 \right] \tag{40a}$$

for the bubble-point (BP) pressure method, and

$$S_{\mathrm{Flash}} = \sum_{i}^{\mathrm{np}} \left[(x_i^{\mathrm{exp}} - x_i^{\mathrm{calc}})^2 + (y_i^{\mathrm{exp}} - y_i^{\mathrm{calc}})^2 \right] \tag{40b}$$

for the flash calculation method is searched using the same optimization method.

In Eq. (40), $(P_i^{\mathrm{exp}} - P_i^{\mathrm{calc}})$, $(x_i^{\mathrm{exp}} - x_i^{\mathrm{calc}})$, and $(y_i^{\mathrm{exp}} - y_i^{\mathrm{calc}})$ are the residuals between the experimental and calculated values of, bubble-point pressures, liquid compositions, and vapor compositions, respectively, for a given experimental point i.

The agreement between calculated and experimental values is evaluated through the standard relative percent deviation in pressure, σ_P, and standard percent deviation in mole fraction

Table 3
Problem 1: C_1 (1)/H_2S (2) at $p = 40.53$ bar and $T = 190$ K; $k_{12} = 0.06$

Feed composition (z_1)	Stationary points of the TPD function (x_1)	Objective function ($\bar{D}$)	Function evaluations	NT	Initialization type	State
0.9885	0.988500	0	493(19)	1	V	Stable
	0.988500	0	479(16)	1	L	
0.9813	0.103160	−0.000789	722(11 + 8 + 7)	2	V	Unstable
	0.914333	−0.008863				
	0.981300	0	924(10 + 4 + 34)	2	L	
	0.914333	−0.008863				
0.93	0.126968	0.091261	611(8 + 28 + 6)	2	V	Stable
	0.930000	0				
	0.930000	0	593(10)	1	L	
0.50	0.102702	−0.066684	753(10 + 9 + 7)	2	V	Unstable
	0.913900	−0.072790				
	0.981253	−0.063764	737(8 + 5 + 26)	2	L	
	0.913900	−0.072790				
0.102	0.102000	0	757(11 + 8 + 7)	2	V	Unstable
	0.913225	−0.003062				
	0.913225	−0.003062	764(8)	1	L	
0.101	0.101000	0	1563(11)	1	V	Stable
	0.912232	0.001343	1628(8 + 13 + 5)	2	L	
	0.101000	0				

Table 4
Problem 2: C_1 (1)/C_3 (2) at $p = 50$ bar and $T = 277.6$ K; $k_{12} = 0.0108$

Feed composition (z_1)	Stationary points of the TPD function (x_1)	Objective function ($\bar{D}$)	Function evaluations	NT	Initialization type	State
0.10	0.100000	0	685(10)	1	V	Stable
	0.100000	0	676(11)	1	L	
0.40	0.400000	0	839(10 + 13 + 10)	2	V	Unstable
	0.865380	−0.149707				
	0.865380	−0.149707	809(9)	1	L	
0.60	0.196827	−0.231321	1586(8)	1	V	Unstable
	0.196827	−0.231321	1573(9)	1	L	
0.90	0.900000	0	984(8)	1	V	Stable
	0.900000	0	979(10)	1	L	

Table 5
Problem 2: C_1 (1)/C_3 (2) at $p = 98$ bar and $T = 277.6$ K; $k_{12} = 0.0108$

Feed composition (z_1)	Stationary points of the TPD function (x_1)	Objective function ($\bar{D}$)	Function evaluations	NT	Initialization type	State
0.40	0.400000	0	1070(10)	1	V	Stable
	0.400000	0	1067(7)	1	L	
0.68	0.669781	−5.656E−7	826(17 + 84 + 5)	2	V	Unstable
	0.738787	−7.435E−5				
	0.669781	−5.656E−7	824(15 + 84 + 5)	2	L	
	0.738787	−7.435E−5				
0.73	0.654521	−3.908E−5	1160(15)	1	V	Unstable
	0.654521	−3.908E−5	1162(13)	1	L	
0.90	0.900000	0	108012)	1	V	Stable
	0.900000	0	1077(9)	1	L	

for the liquid, σ_x, and vapor, σ_y, phases of methane.

$$\sigma_P = 100\left[\frac{1}{\mathrm{np}}\sum_{i}^{\mathrm{np}}\left(\frac{P_i^{\mathrm{exp}} - P_i^{\mathrm{calc}}}{P_i^{\mathrm{exp}}}\right)\right]^{1/2} \tag{41a}$$

$$\sigma_x = 100\left[\frac{1}{\mathrm{np}}\sum_{i}^{\mathrm{np}}(x_i^{\mathrm{exp}} - x_i^{\mathrm{calc}})^2\right]^{1/2} \tag{41b}$$

$$\sigma_y = 100\left[\frac{1}{\mathrm{np}}\sum_{i}^{\mathrm{np}}(y_i^{\mathrm{exp}} - y_i^{\mathrm{calc}})^2\right]^{1/2} \tag{41c}$$

where σ_P, σ_x, and σ_y were obtained by using the optimal values of binary interaction parameters.

Calculations are summarized in Table 2: number of experimental points, temperature and pressure ranges, standard deviations and BIPs, for data from [43,44], and for the whole data set. Examination of the results listed in Table 2 reveals that (i) standard percent deviations σ_P are systematically larger than σ_x and σ_y, (ii) the BIPs calculated with the BP method are larger than those calculated with the flash method, (iii) in terms of temperature dependence, the trend suggested by our calculations is that the BIP decreases as temperature increases, and (iv) σ_y from the BP method are (obviously) larger than those from the flash method, but they still indicated a very good agreement. We suggest the use of BIP values obtained from the BP method.

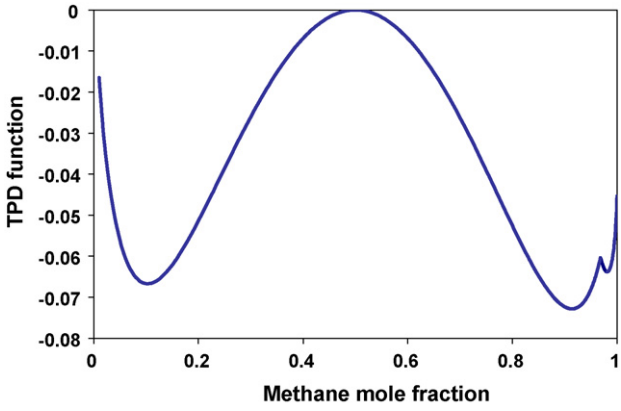

Fig. 3. TPD function for the C_1/H_2S (equimolar) at $p = 40.53$ bar and $T = 190$ K.

Results of phase stability testing of C_1 (1)/H_2S (2) at $p = 40.53$ bar and $T = 190$ K for several feeds are presented in Table 3. Calculations are performed with $k_{12} = 0.06$. For each feed there are given: the stationary points found by tunneling, the value of the objective function, the number of function evaluations (in parenthesis detailed are given for each minimization/tunnelization cycle; FE for the last tunneling phase is given by the difference to total FE), the number of tunneling phases,

Table 6
Problem 3: C_2 (1)/N_2 (2) at $p = 76$ bar and $T = 270$ K; $k_{12} = 0.04134$

Feed composition (z_1)	Stationary points of the TPD function (x_1)	Objective function ($\bar{D}$)	Function evaluations	NT	Initialization type	State
0.90	0.900000	0	879(12)	1	V	Stable
	0.900000	0	881(14)	1	L	
0.82	0.519224	−0.001150	1293(8)	1	V	Unstable
	0.519224	−0.001150	1293(10)	1	L	
0.70	0.501155	−0.015762	826(8)	1	V	Unstable
	0.501155	−0.015762	828(10)	1	L	
0.56	0.560000	0	1121(9 + 26 + 4)	2	V	Unstable
	0.836911	−0.015989				
	0.560000	0	1139(27 + 26 + 4)	2	L	
	0.836911	−0.015989				
0.40	0.400000	0	855(7)	1	V	Stable
	0.400000	0	858(10)	1	L	

and the initialization type (L or V). The last column indicates the state of the mixture at given (T,p,$\mathbf{z}$) conditions (stable, i.e. single phase if $\bar{D}$ is zero at its global minimum, or unstable, i.e. the mixture splits into two or more equilibrium phases if the global minimum of $\bar{D}$ is negative). Fig. 3 plots the TPD function vs. methane mole fraction for the equimolar mixture, showing a local minimum (at $x_1 = 0.9813$) near the global minimum (located at $x_1 = 0.9139$). For one initialization the method finds first the local minimum, and then the global minimum is found by a second minimization, while for the other initialization the global minimum is found by the first minimization. Note that the last two feeds in Table 3 are different from those in [10,15]; there were chosen in the vicinity of the phase boundary, which is crossed at about $z_1 = 0.101$ for the PC-SAFT EoS.

4.2. Problem 2: methane–propane binary mixture

This is a binary mixture of methane (1) and propane (2) at $T = 277.6$ K. The BIP is $k_{12} = 0.0108$, taken from [33]. The results are reported in Table 4 for $p = 50$ bar and in Table 5 for $p = 98$ bar. Feeds 2 and 3 for $p = 98$ bar are close to critical conditions. The TPD function is plot vs. methane mole fraction in Fig. 4a for feed 2 (with 0.68 C_1). A detail is given in Fig. 4b, illustrating the particularities that make this feed difficult: the value of the objective function at the global minimum is very small ($\bar{D} = -7.44\text{E}-5$), and a local minimum (with $\bar{D} = -5.66\text{E}-7$) is located in its vicinity. For both initializations, tunneling finds first the local minimum, then it escapes from its valley in the first tunnelization stage (note the relatively high number of FE in this stage as compared with the other examples), and finds the global minimum in a second minimization.

4.3. Problem 3: ethane–nitrogen binary mixture

This is a binary mixture of ethane (1) and nitrogen (2) at $p = 76$ bar and $T = 270$ K, with $k_{12} = 0.04134$ (the BIP is taken from García-Sánchez et al. [34]). Results for five feeds

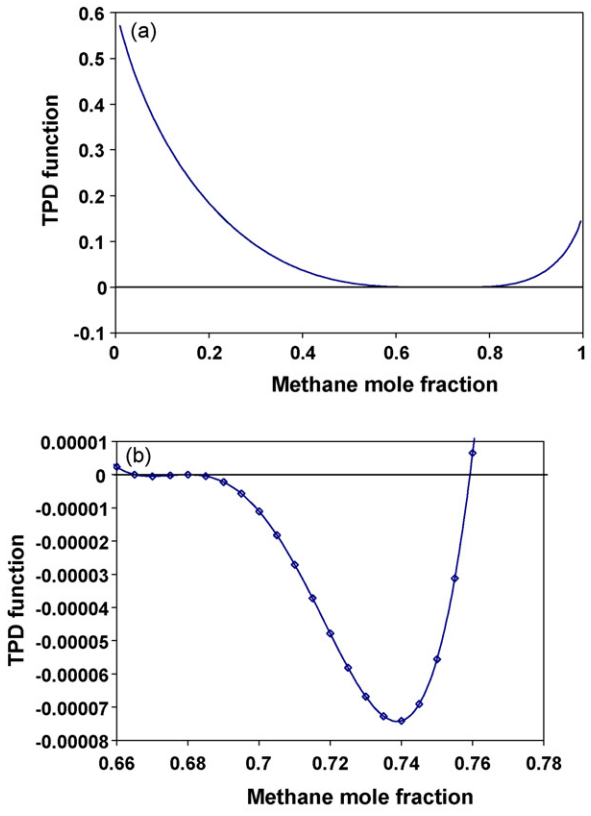

Fig. 4. (a) TPD function for the C_1/C_3 (0.68/0.32) at $p = 98$ bar and $T = 277.6$ K. (b) TPD function for the C_1/C_3 (0.68/0.32) at $p = 98$ bar and $T = 277.6$ K. Detail.

(with feeds 2 and 3 at near saturation conditions) are given in Table 6.

4.4. Problem 4: methane–carbon dioxide binary mixture

This is a binary mixture of methane (1) and carbon dioxide (2) at $p = 60.8$ bar and $T = 220$ K. The BIP is $k_{12} = 0.06$ [33]. The results of stability testing for five feeds are presented in Table 7.

Table 7
Problem 4: C_1 (1)/CO_2 (2) at $p = 60.8$ bar and $T = 220$ K; $k_{12} = 0.06$

Feed composition (z_1)	Stationary points of the TPD function (x_1)	Objective function ($\bar{D}$)	Function evaluations	NT	Initialization type	State
0.90	0.900000	0	836(13)	1	V	Stable
	0.900000	0	833(10)	1	L	
0.80	0.509871	−0.002928	1415(8)	1	V	Unstable
	0.509871	−0.002928	1416(8)	1	L	
0.70	0.569416	−0.001904	754(8 + 17 + 4)	2	V	Unstable
	0.807787	−0.007517				
	0.569416	−0.001904	755(9 + 17 + 4)	2	L	
	0.807787	−0.007517				
0.57	0.570000	0	756(8 + 17 + 5)	2	V	Unstable
	0.807848	−0.005677				
	0.570000	0	757(9 + 17 + 5)	2	L	
	0.807848	−0.005677				
0.40	0.400000	0	1145(10)	1	V	Stable
	0.400000	0	1133(8)	1	L	

Table 8
Problem 5: C_1 (1)/C_2 (2)/N_2 (3) at $p = 76$ bar and $T = 270$ K; $k_{12} = -0.006$, $k_{13} = 0.0307$, $k_{23} = 0.0418$

Feed composition (z_1,z_2)	Stationary points of the TPD function[a]	Objective function ($\bar{D}$)	Function evaluations	NT	Initialization type	State
(0.10,	(0.070855, 0.787534)	−0.013459	3839(12)	1	V	Unstable
0.60)	(0.103344, 0.570830)	−6.329E−5	4186(20 + 165 + 10)	2	L	
	(0.070855, 0.787534)	−0.013459				
(0.30,	(0.305823, 0.537154)	−3.697E−6	4604(21 + 141 + 15)	2	V	Unstable
0.55)	(0.255426, 0.640274)	−7.866E−4				
	(0.305823, 0.537154)	−3.697E−6	4601(18 + 141 + 15)	2	L	
	(0.255426, 0.640274)	−7.866E−4				
(0.38,	(0.38, 0.54)	0	4403(17)	1	V	Stable
0.54)	(0.38, 0.54)	0	4401(15))	1	L	
(0.05,	(0.05, 0.90)	0	4991(14)	1	V	Stable
0.90)	(0.05, 0.90)	0	4980(20)	1	L	

[a] (x_1,x_2).

Table 9
Composition and BIPs for the Y8 mixture

Component	Mole fraction	k_{1j}	k_{2j}
C_1	0.8097	–	
C_2	0.0566	−0.006	–
C_3	0.0306	0.011	0.0015
nC_5	0.0457	0.020	0.005
nC_7	0.0330	0.023	0.008
nC_{10}	0.0244	0.0271	0.010

4.5. Problems 5: methane–ethane–nitrogen ternary mixture

This is a ternary mixture of methane (1), ethane (2) and nitrogen (3) at $p = 76$ bar and $T = 270$ K. The BIPs are $k_{12} = -0.006$ [33], $k_{13} = 0.0307$ [34], and $k_{23} = 0.0418$ [34]. Calculations are performed for four feeds; the results are presented in Table 8. Note that the first feed (unstable) is near dewpoint conditions, while feeds 2 (unstable) and 3 (stable) are at near-critical conditions.

4.6. Problems 6: the Y8 six-component synthetic mixture

Finally, we test phase stability for a six-component synthetic mixture studied by Yarborough [32], referred in the literature as Y8 mixture. This is a model gas condensate containing normal-alkanes (feed composition is given in Table 9). Methane and ethane BIPs from [33] (k_{1j} and k_{2j}, respectively) are listed in Table 8; all other BIPs are set to zero. The dewpoint at $T = 366.5$ K calculated in a predictive mode with the PC-SAFT EoS is 219.27 bar (the experimental value is 216.36 bar [32]). The results of stability testing for four pressures on the $T = 366.5$ K isotherm are given in Table 10.

For problems 1–5, the number of FE required to find the global minimum and to ascertain globality is comparable with the number of FE reported in [15] for TUNPEQ with the PR EoS or SRK EoS. For the last example (with the problem dimensionality $n = 5$), just thousands of FE are required for the selected conditions. We should mention that the tunneling method is designed to search for the global minimum of the objective function, and not for all its stationary points; however, finding all stationary points with tunneling is possible [19] by using a modified objective function for the stability problem (Stateva and Tsvetkov [45]) with multiple global minima at the same level.

Global optimization methods are very costly as compared to local methods. It was established in several publications that tunneling is at least on order of magnitude faster than other global optimization methods for reliably solving various phase equilibrium problems with cubic EoS. The same trend is expected

Table 10
Problem 6: Y8 mixture

(T, K/P, bar)	Objective function ($\bar{D}$)	Function evaluations	NT	Initialization type	State
366.5/200	−0.019679	3686(15)	1	V	Unstable
	0	3271(17 + 11 + 14)	2	L	
	−0.019679				
366.5/219.25	−0.749308E−5	2828(16)	1	V	Unstable
	0	3096(14 + 22 + 8)		L	
	−0.749308E−5		2		
366.5/219.3	0.238929E−4	3618(16 + 79 + 7)	2	V	Stable
	0				
	0	4069(14)	1	L	
366.5/230	0	2775(30)	1	V	Stable
	0	3631(14)	1	L	

for more complex thermodynamic models. Moreover, the use of efficient optimization tools is more stringent if highly complex thermodynamic models are used, since the cost of a single function evaluation is significantly higher.

5. Conclusions

The gradient-based tunneling global optimization method was successfully used for finding the global minimum of the TPD function, using the PC-SAFT EoS (without association) for mixtures containing hydrocarbon components and hydrogen sulphide, carbon dioxide and nitrogen. The tunneling method proved to be reliable and efficient by several difficult numerical experiments. The three H_2S parameters required by the PC-SAFT equation, as well as the BIP between H_2S and methane were calculated by matching available experimental data.

Acknowledgements

DVN would like to thank Prof. Alain Graciaa and Prof. Daniel Broseta of Université de Pau et des pays de l'Adour (UPPA) for their support during this work. We also thank Prof. Jean-Luc Daridon (UPPA) for his interest in this work and useful discussions, and Nelson del Castillo (IIMAS-UNAM) for technical assistance.

References

[1] The Collected Works of J. Willard Gibbs, Yale University Press, New Haven, 1957.
[2] L.E. Baker, A.C. Pierce, K.D. Luks, Soc. Petrol Eng. J. 22 (1982) 731–742.
[3] M.L. Michelsen, Fluid Phase Equilib. 9 (1982) 1–19.
[4] A.C. Sun, W.D. Seider, Fluid Phase Equilib. 103 (1995) 213–249.
[5] C.M. Mc Donald, C.A. Floudas, Thermodynamics 41 (1995) 1798–1814.
[6] C.M. Mc Donald, C.A. Floudas, Ind. Eng. Chem. Res. 34 (1995) 1674–1687.
[7] C.M. Mc Donald, C.A. Floudas, Comp. Chem. Eng. 19 (1995) 1111–1139.
[8] C.M. Mc Donald, C.A. Floudas, Comp. Chem. Eng. 21 (1997) 1–23.
[9] J.Z. Hua, J.F. Brennecke, M.A. Stadtherr, Fluid Phase Equilib. 116 (1996) 52–59.
[10] J.Z. Hua, J.F. Brennecke, M.A. Stadtherr, Ind. Eng. Chem. Res. 37 (1998) 1519–1527.
[11] J.Z. Hua, J.F. Brennecke, M.A. Stadtherr, Fluid Phase Equilib. 158–160 (1999) 607–615.
[12] G.I. Burgos-Solorzano, J.F. Brennecke, M.A. Stadtherr, Fluid Phase Equilib. 219 (2004) 245–255.
[13] Y. Zhu, H. Wen, Z. Xu, Chem. Eng. Sci. 55 (2000) 3451–3459.
[14] J. Balogh, T. Csendes, R.P. Stateva, Fluid Phase Equilib. 212 (2003) 257–267.
[15] D.V. Nichita, S. Gómez, E. Luna, Comp. Chem. Eng. 26 (2002) 1703–1724.
[16] D.V. Nichita, S. Gómez, E. Luna, Fluid Phase Equilib. 194–197 (2002) 411–437.
[17] D.V. Nichita, S. Gómez, E. Luna, J. Can. Petrol. Technol. 43 (2004) 13–16.
[18] D.V. Nichita, S. Gómez, C. Duran-Valencia, Chem. Eng. Commun. 193 (2006) 1194–1216.
[19] D.V. Nichita, S. Gómez, Comp. Chem. Eng. (submitted for publication).
[20] W.G. Chapman, G. Jackson, K.E. Gubbins, Mol. Phys. 65 (1988) 1057–1079.
[21] E.A. Müller, K.E. Gubbins, Ind. Eng. Chem. Res. 40 (2001) 2193–2211.
[22] J. Gross, G. Sadowski, Ind. Eng. Chem. Res. 40 (2001) 1244–1260.
[23] N. van Solms, M.L. Michelsen, G.M. Kontogeorgis, Ind. Eng. Chem. Res. 42 (2003) 1098–1105.
[24] S.S. Chen, A. Kreglewski, Ber. Bunsenges. Phys. Chem. 81 (1977) 1048–1052.
[25] A.V. Levy, A. Montalvo, SIAM J. Sci. Stat. Comp. 1 (1985) 15–29.
[26] C. Barrón, S. Gómez, The exponential tunneling method. Technical Report 3, IIMAS, UNAM, 1991.
[27] S. Gómez, J. Solano, L. Castellanos, M.I. Quintana, Advances in Convex Analysis and Global Optimization, Kluwer Academic Publishers, 2001.
[28] R.H. Byrd, P. Lu, J. Nocedal, C. Zhu, SIAM J. Sci. Comput. 16 (1995) 1190–1208.
[29] C. Zhu, R.H. Byrd, P. Liu, J. Nocedal, ACM T. Math. Software 23 (1997) 550–560.
[30] J. Nocedal, S.J. Wright, Numerical Optimization, Springer, 1999.
[31] P. Gill, W. Murray, M. Wright, Practical Optimization, Academic Press, 1981.
[32] L. Yarborough, J. Chem. Eng. Data 17 (1972) 129–133.
[33] F. García-Sánchez, D.V. Nichita, The 16th International Congress of Chemical and Process Engineering CHISA2004, Prague, August 22–26, 2004.
[34] F. García-Sánchez, G. Eliosa-Jiménez, G. Silva-Oliver, R. Vázquez-Román, Fluid Phase Equilib. 217 (2004) 241–253.
[35] Wilson, G., Paper No. 15C presented at the AIChE 65th National Meeting, Cleveland, OH, May 4–7, 1969.
[36] R.C. Reid, J.M. Prausnitz, B.E. Poling, The Properties of Gases and Liquids, McGraw-Hill, Singapore, 1988.
[37] J.A. Nelder, R.A. Mead, Comput. J. 7 (1965) 308–313.
[38] J.H. Wegstein, Commun. ACM 1 (1958) 9–13.
[39] W.B. Kay, G.M. Rambosek, Ind. Eng. Chem. 45 (1953) 221–226.
[40] J.A. Bierlien, W.B. Kay, Ind. Eng. Chem. 45 (1953) 618–624.
[41] M.A. Gomez-Nieto, C.G. Papadopoulos, Technical Report, Northwestern University, Evanston, Illinois, 1976.
[42] T.E. Daubert, R.P. Danner, Physical and Thermodynamic Properties of Pure Compounds: Data Compilation, Hemisphere, New York, 2001.
[43] H.H. Reamer, B.H. Sage, W.N. Lacey, Ind. Eng. Chem. 43 (1951) 976–981.
[44] J.P. Kohn, F. Kurata, AIChE J. 4 (1958) 211–217.
[45] R.P. Stateva, S.G. Tsvetkov, Can. J. Chem. Eng. 72 (1994) 722–734.